

Effects of vagal blockade on the complexity of heart rate variability in rats

M. Baumert¹, E. Nalivaiko² and D. Abbott¹

¹ Centre for Biomedical Engineering, School of Electrical and Electronic Engineering, The University of Adelaide, Adelaide, Australia;

² Department of Human Physiology and Centre for Neuroscience, Flinders University, Adelaide, Australia.

Abstract— In this paper we investigate the influence of vagal blockage on heart rate variability complexity measures. Nine conscious rats are injected with methyl-scopolamine bromide (50 µg/kg s.c.). We analyze 10 minute segments of beat-to-beat intervals before and after injection by standard time and frequency domain methods, compression entropy, sample entropy, Poincaré plot, detrended fluctuation analysis and symbolic dynamics. All parameter domains show changes in heart rate variability after vagal blockade, indicating a decrease in heart rate complexity. In conclusion, vagal modulation plays an important role in the generation of heart complexity in rats or, in other words, heart rate complexity measures are sensitive to vagal heart rate modulation.

Keywords— heart rate variability, complexity, vagal blockade, rat

I. INTRODUCTION

The heart rate underlies beat-to-beat variations, reflecting modulations mediated by vagal and sympathetic branches of the autonomic nervous system. Heart rate variability (HRV) analysis has shown prognostic significance in patients after acute myocardial infarction [1] and in the diagnosis of autonomic neuropathy [2]. Furthermore, it is used in various research settings such as sports [3] or obstetrics [4].

The quantification of HRV is basically a time series analysis task, and numerous approaches have been proposed, including traditional time and frequency domain measures [5], but also measures from complex systems science [4,6,7,8]. Although the sensitivity of some of those new measures often appeared superior to standard time and frequency domain measures, their physiological meaning is hardly understood and their interpretation remains difficult.

To assess their sensitivity to vagal heart rate modulation we investigate the impact of vagal blockade on HRV complexity measures in a rat model.

II. METHODS

A. Animal preparation and experimental protocol

The study is performed on nine male Wistar Hooded rats weighing 250-300 g. Experiments are conducted in accor-

dance with the European Community Council Directive of 24 November 1986 (86/609/EEC), and are approved by the Flinders University Animal Welfare Committee. During preliminary surgery, telemetric ECG transmitters (TA11CA-F40, Data Science International, USA) are implanted into the peritoneal cavity under isoflurane (1.5% in 100% oxygen) anesthesia. On the day of experiment, ECG is recorded before and after administration of methyl-scopolamine bromide (50 µg/kg s.c., Sigma, USA), a vagal blocker that does not cross blood-brain barrier. Analogue signal is acquired using the MacLab interface and Chart software (ADInstruments, Sydney, Australia).

B. Heart rate variability analysis

Pre-processing: RR intervals series are extracted from the ECG recording, using the Chart® software (ADInstruments, Sydney, Australia). Subsequently, RR time series are scanned and manually edited. Artifacts and ectopic beats are filtered, resulting in a normal-to-normal (NN) interval time series. For further analysis we select a segment of a 10 minute length, starting 15 minutes prior to the vagal blockade injection in order to obtain HRV baseline values. To analyze HRV during vagal blockade, we select ten minute epochs, beginning five minutes after injection.

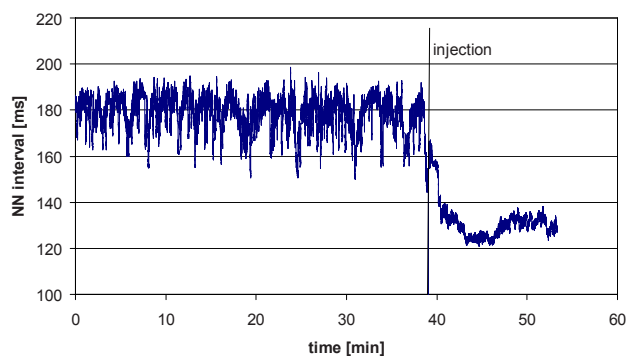


Fig. 1 Beat-to-beat interval time series in a conscious rat prior and after injection of methyl-scopolamine. The NN interval as well as heart rate variability decreases.

Time domain analysis: For traditional time domain analysis of HRV we compute $meanNN$, the mean beat-to-beat interval of normal heart beats, its standard deviation $sdNN$, and the root-mean-square of successive beat-to-beat differences $rmssd$.

Frequency domain analysis: For frequency domain analysis of HRV we generate equidistant time series, using a linear interpolation at 20 Hz. Subsequently, the power spectrum is estimated, using FFT and a Blackman-Harris window. Total power (P : 0-3Hz), very low frequency power (VLF : 0.03-0.25 Hz), low frequency power (LF : 0.25-1 Hz) as well as high frequency power (HF : 1-3 Hz) are computed.

Poincaré plots: Poincaré plots provide a visual way to study dynamics underlying HRV. As commonly used, NN intervals are plotted against the previous ones (i.e. NN_{n+1} vs. NN_n). Although this approach is somewhat simplified with regard to the non-linear systems theoretical intention, it is a useful tool for HRV analysis. Usually, an ellipsoid shape is fitted to the points and the short axis $SD1$ and long axis $SD2$ are taken as measures. Although the Poincaré plot itself may capture non-linear characteristics of HRV, $SD1$ as well as $SD2$ capture only linear characteristics [9].

Compression entropy: To study the short-term complexity of beat-to-beat fluctuations we recently introduced a compression based complexity measure [8]. From the point of information theory, the smallest algorithm that produces a string is the entropy of that string (Chaitin-Kolmogorov entropy). Although it is theoretically impossible to develop such an algorithm, data compression techniques might provide a good approximation. We apply a modified version of the LZ77 algorithm for lossless data compression introduced by Lempel and Ziff in 1977 [10]. The algorithm is based on a sliding window technique and searches for matching sequences. It keeps the w , the most recently encoded source symbols (sliding window of size w). The not-yet-encoded sequence of symbols is stored in the look-ahead buffer of size b . The encoder positioned at p looks for the longest match of length n between the not-yet-encoded n -string x_p^{p+n-1} in the look-ahead buffer and the already encoded string $x_{p-w+v}^{p-w+v+n-1}$ in the window beginning at position v . Thus, the matching string of n symbols is simply encoded by encoding the integer numbers n and v , i.e. a pointer to the previous occurrence of this string in the sliding window. Then the position and length of the matching sequence are stored. The ratio of the uncompressed to the compressed file, called compression entropy H_c , is used as complexity measure. We set $b = 3$ and $w = 7$ as previously published [8].

Symbolic Dynamics: The concept of symbolic dynamics allows a simplified description of the dynamics of a system with a limited amount of symbols. Methods based on symbolic dynamics have already been successfully applied to HRV analysis providing some more global information about the underlying system. In this study we employ the technique proposed by Voss *et al.* [6]. The difference between each NN interval and mean NN is transformed into an alphabet of 4 symbols $\{0, 1, 2, 3\}$. Symbols '0' and '2' reflect low deviation (decrease or increase) from the mean NN interval, whereas '1' and '3' reflect a stronger deviation (decrease or increase over a predefined limit). Subsequently, the symbol string is transformed to words (bins) of three successive symbols. The distribution of word types reflects some nonlinear properties of HRV (see [6] for detailed information). From this symbolic dynamics the following parameters are calculated: $WPSUM13$: words that contain only symbols '1' and '3' reflecting high variability; $WPSUM02$: words that contain only symbols '0' and '2' reflecting high variability; $FORWORD$: number of word types that occur seldom, i.e. with a probability less 0.001.

Using a modified symbol transformation consecutive NN differences less than 2 ms are coded as '0' and otherwise as '1'. In this way two further parameters are obtained: $PLVAR2$: percentage of words of length 6 that contain only '0', reflecting a low variability; $PHVAR2$: percentage of words of length 6 that contain only '1', reflecting a high variability.

Sample entropy: Sample entropy ($SampEn$) calculates the probability that epochs of window length m that are similar within a tolerance r remain similar at the next point. $SampEn$ is precisely the negative natural logarithm of the conditional probability that a dataset of length N , having repeated itself within a tolerance r for m points, will also repeat itself for $m + 1$ points, without allowing self-matches. In agreement with previously published studies we choose values of $r = 0.25$ and $m = 2$ [4].

Detrended fluctuation analysis: The DFA technique has been developed to analyze long-range correlations (long-memory dependence) in non-stationary data, where conventional fluctuation analyses such as power spectra and Hurst analysis cannot be reliably used [7]. The method works as follows:

1. Compute the cumulative sum $c(k) = \sum_{i=1}^k [s(i) - \bar{s}]$ of the time series s where \bar{s} is the mean of S (using the concept of Random-Walk-Analysis).
2. Compute the local trend $c_n(k)$ within boxes of varying sizes n (least square fit).
3. Compute the root mean square of the detrended time series in dependency on box size n as

$$F(n) = \sqrt{\frac{1}{N} \sum_{k=1}^N [c(k) - c_n(k)]^2}, \text{ where } N \text{ denotes the size}$$

of S .

4. Plot $\log_{10} F(n)$ against $\log_{10} n$.

If the data displays long-range dependence then $F(n) \sim n^\alpha$, where α is the scaling exponent. For stationary data with scale-invariant temporal organization, the Fourier power spectrum $S(f)$ is $S(f) \sim f^{-\beta}$, where the scaling exponent β is related to α in the following way: $\beta = 2\alpha - 1$. Values of $0 < \alpha < 0.5$ are associated with anti-correlation (i.e. large and small values of the time series are likely to alternate). For Gaussian white noise $\alpha = 0.5$. Values of $0.5 < \alpha \leq 1$ indicate long-range power-law correlations (i.e. large values of the time series are likely to be followed by large values). Values $1 < \alpha \leq 1.5$ represent stronger long-range correlations that are different from power-law where $\alpha = 1.5$ for Brownian motion. We compute two scaling exponents, α_{LF} and α_{VLF} that are related to the LF and VLF frequency ranges as defined above. In order to estimate frequency values f_n from the segment size n of DFA, in Hertz, the segment sizes are related to the mean heart rate ($meanNN^{-1}$), i.e. $f_n \approx meanNN^{-1}n$ [11].

Table 1 Heart rate variability measured in nine rats before (baseline) and after injection of methyl-scopolamine (vagal blockade) displayed as medians and inter-quartile ranges as well as p-values of the Wilcoxon test for paired comparisons of medians

HRV measure	baseline	vagal blockade	p
meanNN	179 [178 – 198]	144 [131 – 155]	0.0039
sdNN	7.6 [5.0 – 10.1]	4.3 [4.0 – 5.0]	0.098
Rmssd	2.5 [2.1 – 2.9]	0.8 [0.8 – 1.0]	0.0039
P	33.9 [15.8 – 45]	13.6 [8.6 – 21.7]	0.30
VLF	7.2 [6.2 – 11.9]	1.7 [1.1 – 2.3]	0.0039
LF	1.54 [0.74 – 2.33]	0.11 [0.10 – 0.18]	0.0039
HF	1.63 [0.90 – 2.33]	0.22 [0.21 – 0.32]	0.0039
H_c	0.41 [0.39 – 0.43]	0.31 [0.30 – 0.31]	0.0039
SD1	1.8 [1.5 – 2.1]	0.6 [0.5 – 0.7]	0.0039
SD2	10.6 [7.0 – 14.3]	6.1 [5.6 – 7.1]	0.098
WPSUM13	0.11 [0.04 – 0.24]	0.06 [0.04 – 0.18]	0.57
WPSUM20	0.73 [0.58 – 0.94]	0.92 [0.75 – 0.92]	0.30
FORWORD	42 [42 – 42]	42 [42 – 44]	1
PLVAR2	0.15 [0.04 – 0.17]	0.94 [0.87 – 0.96]	0.0039
PHVAR2	0.016 [0.003 – 0.024]	0.000 [0.000 – 0.000]	0.0039
SampEn	1.00 [0.84 – 1.19]	0.42 [0.33 – 0.73]	0.074
α_{LF}	0.96 [0.85 – 1.04]	1.01 [0.98 – 1.18]	0.16
α_{VLF}	1.31 [1.22 – 1.34]	1.41 [1.38 – 1.44]	0.0039

III. RESULTS

After injection of methyl-scopolamine, a vagal blocker, the heart rate increases, i.e. $meanNN$ reduces in all rats. Fig.1 shows an example of the NN interval time series before and after injection. For statistical comparison of HRV measures we compute group medians, inter-quartile ranges as well as the Wilcoxon test. Results are summarized in Tab.1.

The overall HRV, as measured in the time domain via $sdNN$, is reduced in trend, but does not reach statistical significance. A more detailed analysis of HRV reveal drastically reduced beat-to-beat variability ($rmssd$). The frequency domain analysis shows that the high (HF), low frequency (LF), and very low frequency (VLF) power is reduced, whereas the overall power is decreased in trend only.

The Poincaré plot based analysis shows significantly reduced short-term fluctuations ($SD1$) and nearly significant reduction in $SD2$.

The compression entropy is also significantly reduced after vagal blockade.

Symbolic dynamics based analysis reveals an increase of low variability patterns ($PLVAR2$) paralleled by a decrease in high variability patterns ($PHVAR2$), whereas the other parameters are not significantly changed.

The sampling entropy is reduced after vagal blockade, but does not reach statistical significance.

Scaling analysis by means of DFA shows increased correlations after vagal blockade in the VLF range.

IV. DISCUSSION

In this paper we study HRV, particularly its complexity measures, and changes in these measures caused by vagal blockade in conscious rats. It is well known that vagal blockade leads to an increase in heart rate paralleled by a decrease in variability in the high frequency range [12]. Little is known, however, about the effect of vagal blockade on the complexity of HRV or, in other words, about the sensitivity of complexity measures to vagal modulation of the heart rate. Our data shows the typical increase in heart rate paralleled by a decrease in HRV after vagal blockade. Besides the decrease in HF and $rmssd$ we find LF oscillations to be almost vanished, suggesting that without external stress, LF fluctuations in heart rate are almost completely caused by vagal mechanisms. But also the VLF oscillations are significantly reduced during vagal blockade.

This broad reduction in HRV also affects most of the complexity measures, showing a decreased complexity. The compression based measure H_c assesses fluctuations of

heart rate within a short time window and is therefore sensitive to vagal modulations. Looking at the Poincaré plot, $SD1$ reflects beat-to-beat changes that are exclusively mediated by the vagal pathway whereas, $SD2$ assesses also slower dynamics that might be caused by other regulatory systems, external stimuli or animal's movements, and consequently shows less sensitivity to vagal modulations.

The contradictory behavior of the Symbolic Dynamics measures $PLVAR2$ and $PHVAR2$ that assess beat-to-beat dynamics over 7 consecutive heart beats also reflect the low HRV after vagal blockade. In particular there are no more heart rate patterns with consecutive beat-to-beat changes higher than 2 ms ($PHVAR2$).

Sampling entropy is less sensitive to vagal blockade since this regularity statistic is based on the overall variability of the NN time series that is also influenced by slow trends that are not caused by vagal modulations.

The DFA shows a steeper slope in the VLF range and therefore increased long-range correlations after vagal blockage, which also suggest that vagal modulations cause a certain amount of irregularity in HRV and consequently a vagal blockade is leading to a more regular behavior at larger scales.

Given that heart rate modulations mediated by vagal efferents mainly reflect cardio-respiratory coupling it could be speculated that the irregularity of respiration, including factors such as respiratory frequency, tidal volume, ratio between inspiration and respiration, etc. is the major source of the complexity found and assessed with the above described measures. This emphasizes the necessity of recording respiration in HRV analysis studies.

V. CONCLUSIONS

Vagal blockade of heart rate control in rats shows the typical increase in heart rate paralleled by a decrease in HRV. Several complexity measures are decreased and are therefore sensitive to vagal heart rate modulation.

ACKNOWLEDGMENT

This study was supported by grants from the Australian Research Council (DP0663345).

REFERENCES

1. Kleiger RE, Miller JP, Bigger JT et al. (1987) Decreased heart rate variability and its association with increased mortality after acute myocardial infarction. *Am J Cardiol* 59:256-262
2. Vinik AI, Maser RE, Mitchel BD et al. (2003) Diabetic autonomic neuropathy. *Diabetes Care* 26:1553-1579
3. Baumert M, Brechtel L, Lock J et al (2006) Heart Rate Variability, Blood Pressure Variability, and Baroreflex Sensitivity in Overtrained Athletes. *Clin J Sport Med* 16:412-417
4. Lake DE, Richman JS, Griffin MP et al. (2002) Sample entropy analysis of neonatal heart rate variability. *Am J Physiol Regul Inter Comp Physiol* 283:R789-R797
5. Task Force of the European Society for Cardiology and the North American Society of Pacing and Electrophysiology (1996) Heart rate variability. Standards of measurement, physiological interpretation, and clinical use. 17:354-381
6. Voss A, Kurths J, Kleiner HJ et al. (1996) The application of methods of nonlinear dynamics for the improved and predictive recognition of patients threatened by sudden cardiac death. 31:419-433
7. Peng CK, Havlin S, Stanley HE et al (1996) Quantification of scaling exponents and crossover phenomena in nonstationary heartbeat time series. *Chaos* 5:82-87
8. Baumert M, Baier V, Hauelsen J et al. (2004) Forecasting of Life Threatening Arrhythmias Using the Compression Entropy of Heart Rate. *Methods Inf Med* 43:202-206
9. Brennan M, Palaniswami M, Kamen P (2001) Do existing measures of Poincaré plot geometry reflect nonlinear features of heart rate variability? *IEEE Trans Biomed Eng* 48:1342-1347
10. Ziv J, Lempel A (1977) A universal algorithm for sequential data compression. *IEEE Trans Inf Theory* 23:337-343
11. Baumert M, Brechtel LM, Lock J et al. (2006) Scaling graphs of heart rate time series in athletes demonstrating the VLF, LF and HF regions. *Physiol Meas* 27:N35-N39
12. Japundzic N, Grichois ML, Zitoun P et al. (1991) Spectral analysis of blood pressure and heart rate in conscious rats: effects of autonomic blockers. *J Auton Nerv Syst* 30:91-100

Author: Dr Mathias Baumert

Institute: School of Electrical and Electronic Engineering,
The University of Adelaide

City: Adelaide, SA5005

Country: Australia

Email: mbaumert@eleceng.adelaide.edu.au